Accepted Manuscript

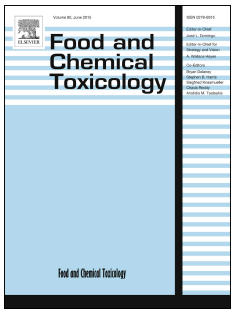

P53 tumor suppressor is required for efficient execution of the death program following treatment with a cytotoxic limonoid obtained from *Melia azedarach*

Mariana Belén Joray, Florencia Villafañez, María Laura González, María Inés Crespo, Jerónimo Laiolo, Sara María Palacios, José Luis Bocco, Gastón Soria, María Cecilia Carpinella

PII: S0278-6915(17)30217-X

DOI: 10.1016/j.fct.2017.04.039

Reference: FCT 9024

To appear in: *Food and Chemical Toxicology*

Received Date: 29 March 2017

Revised Date: 26 April 2017

Accepted Date: 28 April 2017

Please cite this article as: Joray, Mariana.Belé., Villafañez, F., González, Marí.Laura., Crespo, Marí.Iné., Laiolo, Jeró., Palacios, Sara.Marí., Bocco, José.Luis., Soria, Gastó., Carpinella, Marí.Cecilia., P53 tumor suppressor is required for efficient execution of the death program following treatment with a cytotoxic limonoid obtained from *Melia azedarach*, *Food and Chemical Toxicology* (2017), doi: 10.1016/j.fct.2017.04.039.

Graphical Abstract

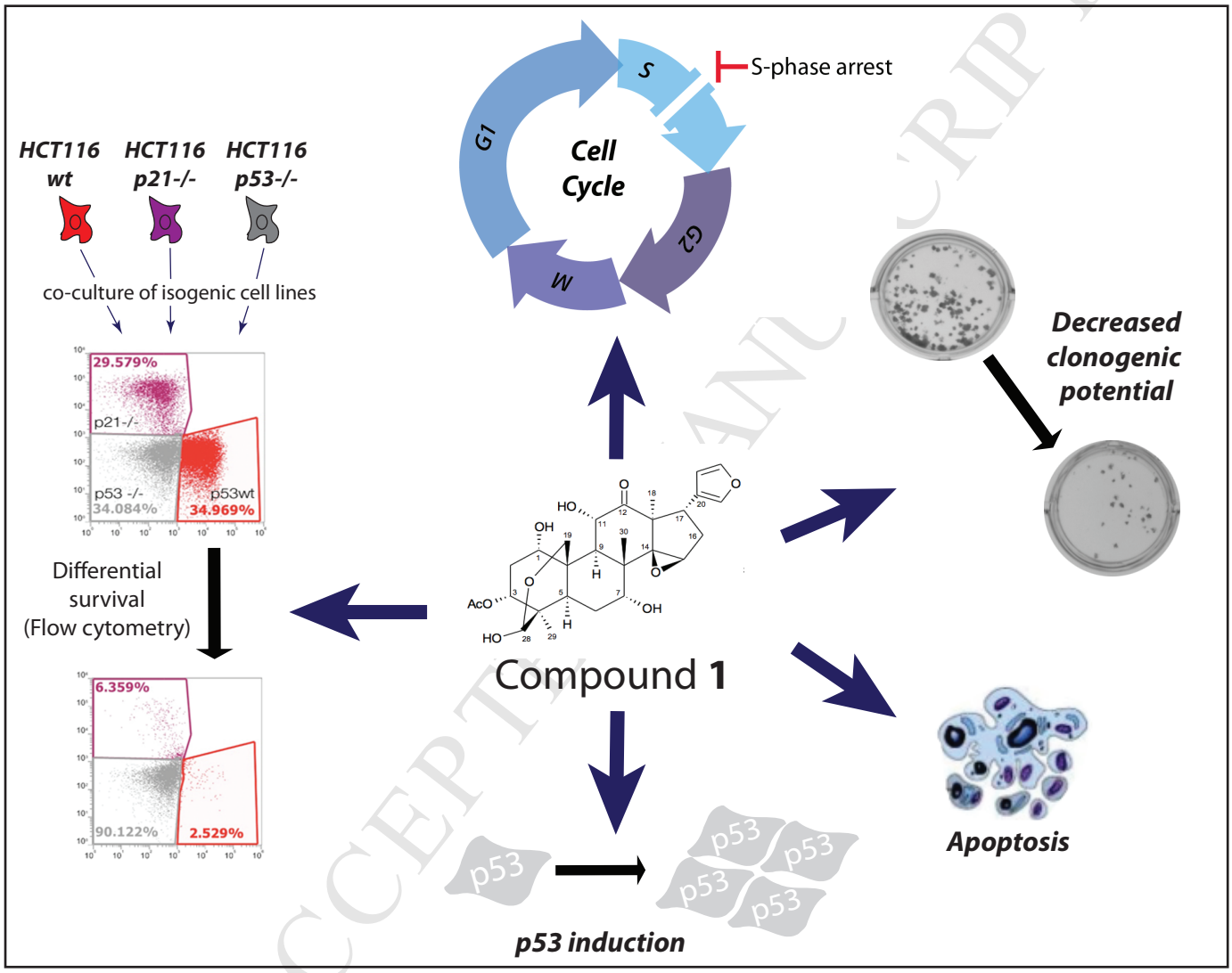

P53 tumor suppressor is required for efficient execution of the death program following treatment with a cytotoxic limonoid obtained from *Melia azedarach*.

Mariana Belén Joray[a], Florencia Villafañez[b], María Laura González[a], María Inés Crespo[a], Jerónimo Laiolo[a], Sara María Palacios[a], José Luis Bocco[b], Gastón Soria[b,*] and María Cecilia Carpinella[a,*]

[a] Fine Chemicals and Natural Products Laboratory, School of Chemistry, Catholic University of Córdoba, Avda Armada Argentina 3555, X5016DHK Córdoba, Argentina.

[b] CIBICI CONICET and Department of Clinical Biochemistry, Faculty of Chemical Science, National University of Córdoba, Haya de la Torre and Medina Allende, Córdoba, Argentina.

Corresponding author: ceciliacarpinella@ucc.edu.ar; cecicarpi@yahoo.com

[1] Laboratorio de Química Fina y Productos Naturales, Facultad de Ciencias Químicas, Universidad Católica de Córdoba, Avda. Armada Argentina 3555, X5016DHK, Córdoba, Argentina. Tel: 54 351- 4938000. Ext 611. Fax: 54 351-4938061.

Corresponding author: gsoria29@gmail.com; gsoria@fcq.unc.edu.ar

[2] CIBICI CONICET and Department of Clinical Biochemistry, Faculty of Chemical Science, National University of Córdoba, Haya de la Torre and Medina Allende, Córdoba, Argentina. Tel: 54 351- 4938000. Ext 611. Fax: 54 351-4938061.

Abstract

This work examines the antitumor activity of an isomeric mixture (**1**), composed of the limonoids meliartenin and its interchangeable isomer 12-hydroxyamoorastatin. The results obtained showed that **1** displayed outstanding cytotoxic activity against CCRF-CEM, K562, A549 and HCT116 cells, with a highly selective effect on the latter, with an IC_{50} value of 0.2 μM. Based on this finding, HCT116 cells were selected to study the mechanism of action of **1**. Cell cycle analysis revealed that **1** induced sustained arrest in the S-phase, which was followed by the triggering of apoptotic cell death and reduced clonogenic capacity. This cytotoxicity was seen to be preceded by the upregulation of the tumor suppressor p53 and its target effector p21. In addition, it was found that p53 expression was required for efficient cell death induction, and thus that the toxicity of **1** relies mainly on p53-dependent mechanisms. Taken together, these findings position **1** as a potent antitumor agent, with potential for the development of novel chemotherapeutic drugs based on the induction of S-phase arrest.

*Keywords***:** meliartenin; 12-hydroxyamoorastatin; cytotoxicity; apoptosis; cell cycle arrest; HCT116; p53.

Abbreviations: ALL, acute lymphoblastic leukemia; BrdU, 5-bromo-2'-deoxyuridine; CML, chronic myeloid leukemia; DMSO, dimethyl sulfoxide; DOX, doxorubicin; FBS, fetal bovine serum; HU, hydroxyurea; MTT, 3-(4,5-Dimethyl-2-thiazolyl)-2,5-diphenyl-2H-tetrazolium bromide; PBS, Phosphate saline buffer; PBSTB, Phosphate saline buffer, tween and fetal bovine albumin; PCNA, proliferating cell nuclear antigen; PI, propidium iodide; pRB, retinoblastoma protein.

Highlights

- The isomeric mixture (**1**) is composed of meliartenin and its interchangeable isomer 12-hydroxyamoorastatin.
- Compound **1** showed a strong cytotoxic effect against a panel of human tumor derived cell lines.
- Compound **1** induced sustained S-phase cell cycle arrest.
- Compound **1** induced apoptosis and decreased clonogenic potential.
- Wild-type p53 expression was required for efficient cell death induction.

1. Introduction

Cancer is the second leading cause of death worldwide. Approximately 14 million new cases were reported in 2012 and 8.8 million deaths occurred in 2015 due to this disease (Ferlay et al., 2015). Factors such as high costs, side effects and the therapeutic limitations of conventional chemotherapeutic drugs mean that there is an urgent need to develop new active selective anticancer agents.

The effectiveness and the diversity of structures of plant-derived metabolites are driving their resurgence as an important source of molecules for drug discovery (Balunas and Kinghorn, 2005; Kristanc and Kreft, 2016).

Despite great advances in the field of plant-drug discovery, the plant world remains largely unexplored in some geographical areas, as in the case of flora from Argentina (Joray et al., 2015). The genus *Melia* is well-known as a rich and valuable source of bioactive tetranortriterpenoids known as limonoids (Zhao et al., 2010). These compounds are formed from the loss of the four terminal carbons of the side chain of the apo-tirucallol or apo-euphol skeleton, resulting in a β-substituted furanyl ring at C-17 (Tan and Luo, 2011). In previous research conducted by our group, the fractionation of a kernel extract obtained from *Melia azedarach* L. led to the isolation of meliartenin, an antifeedant limonoid, which exists as a mixture with its tautomeric isomer 12-hydroxyamoorastatin (Carpinella et al., 2002). The cytotoxicity of 12-hydroxyamoorastatin, in terms of its half- inhibitory concentration (IC_{50}) against a few tumor cell lines, has been previously reported (Ahn et al., 1993; Itokawa et al., 1995; Polonsky et al., 1979). However, despite its potential as an antitumor drug, the mechanistic details involved in its biological effect together with meliartenin, have not yet been explored.

Many proteins have been described as playing a dual role in cell cycle control and apoptosis (Foster, 2008). Among them, p53 is a ubiquitous transcription factor that has an essential role in protecting the cell from multiple stressors (Gottifredi et al., 2001a). P53 exerts many of its functions as a transcriptional activator and repressor by regulating the expression of a number of genes that control cell cycle, cell death, and other cellular functions (Brown et al., 2009; Gottifredi et al., 2001b). The protein $p21^{WAF1}$ (hereafter p21) is a key downstream effector of p53 which modulate cyclin/CDK activity, pRB degradation and PCNA inhibition, thus leading to the activation of the G1/S and S-phase checkpoints (Mirzayans et al., 2012).

In this study, the antitumor activity of the interchangeable isomeric mixture (hereafter **1**) of meliartenin and 12-hydroxyamoorastatin was evaluated over a panel of human tumor-derived cell lines, resulting in a cytotoxic effect that was highly selective of the human colorectal carcinoma cell line HCT116 over the rest of the assayed cell lines. Mechanistic analysis revealed that **1** induced cell cycle arrest and triggered apoptotic cell death at the same time as it decreased the clonogenic potential of the cells. It was also demonstrated that these effects were mediated by the upregulation of the expression of p53 and p21, and that wild-type p53 expression was required for cell death induction. In light of these findings, the present study sets the ground for the potential use of compound **1** for the development of novel anticancer drugs.

2. Materials and methods

2.1. Chemicals, equipment and reagents

The isomeric mixture (**1**) of meliartenin and 12-hydroxyamoorastatin (Fig. 1)

was isolated from Argentine *M. azedarach* fruits (Carpinella et al., 2002). 3-(4,5-dimethylthiazol-2-yl)-2,5-diphenyltetrazolium bromide (MTT), propidium iodide (PI), 5-bromo-2'-deoxyuridine (BdrU), RNase A and hydroxyurea (HU) were purchased from Sigma-Aldrich CO (St Louis, MO). Doxorubicin hydrochloride 99.8% (DOX, Synbias Pharma Ltd.) was purchased from Nanox Release Technology (Buenos Aires, Argentina). SYTOX Red was obtained from Invitrogen Life Technologies (Carlsbad, CA) and Annexin V was purchased from BD Biosciences (San Jose, CA). Sterile plastic material was purchased from Greiner Bio-One (Frickenhausen, Germany). Flow cytometry analysis was performed in a Becton-Dickinson (BD) FACSCanto II (BD Biosciences, San Jose, CA) and in an Attune NxT (Invitrogen Life Technologies (Carlsbad, CA) flow cytometer.

2.2. Cell lines and culture conditions

K562 chronic myeloid leukemia (CML) (Rumjanek et al., 2013) and CCRF-CEM acute lymphoblastic leukemia (ALL) (Efferth et al., 2002) cells were a generous gift from Dr. V. Rumjanek (Institute of Medical Biochemistry Leopoldo de Meis, Universidade Federal do Rio de Janeiro, Rio de Janeiro, Brasil) and Dr. T. Efferth (Institute of Pharmacy and Biochemistry, Johannes Gutenberg University, Mainz, Germany), respectively. Human lung and colorectal cancer cells, A549 and HCT116 respectively, were purchased from American Type Culture Collection (ATCC, Rockville, USA). Leukemic cells were grown in RPMI 1640 medium (Invitrogen Life Technologies, Carlsbad, CA) while the adherent cell lines were grown in DMEM (Invitrogen Life Technologies, Carlsbad, CA), both media supplemented with 10% heat-inactivated fetal bovine serum (FBS), 2 mM glutamine (Invitrogen Life

Technologies, Carlsbad, CA) and penicillin (100 units/mL)-streptomycin (100 µg/mL) (Invitrogen Life Technologies, Carlsbad, CA), at 37°C in a 5% CO_2 humidified environment. Cells were sub-cultured twice a week and used when under 20th passage from frozen stocks. All experiments were performed with cells in the logarithmic growth phase with cell viabilities over 90%, determined by staining with trypan blue. Isogenic $p53^{-/-}$ and $p21^{-/-}$ cell lines were established by knocking out the p53 and p21 genes by homologous recombination (Bunz et al., 1998; Waldman et al., 1995).

2.3. Cell proliferation assay

The MTT colorimetric assay was performed as previously described (Joray et al., 2015). Briefly, 2 x 10^4 adherent cells suspended in 100 µL of complete growth medium were seeded in 96-well plates. After 24 h, 100 µL of medium was added in the presence of serial two-fold dilutions of compound **1** (0.0003-37.5 µM) previously dissolved in acetonitrile (1% v/v since no adverse effects were observed at this concentration). In the case of leukemic cells, 5 x 10^4 cells suspended in 100 µL of growth medium were seeded in 96-well plates containing 100 µL of medium in the presence of serial two-fold dilutions of **1** previously dissolved in acetonitrile. After 72 h incubation, 20 µL of 5 mg/mL solution of MTT in sterile PBS was added to each well and further incubated for 4 h at 37°C. Then, the supernatants were removed and replaced with 100 µL DMSO to solubilize the resulting purple formazan crystals produced from metabolically viable cells. Absorbance was measured with an iMark micro-plate reader (Bio-Rad, USA) at 595 nm. The chemotherapeutic DOX dissolved in sterile water (0.001-34.5 µM) and 1% acetonitrile were used as positive and negative controls, respectively. The percentage of cytotoxic activity of the assayed compound

was determined by use of the following formula: Cytotoxicity (%) = [1- (Optical density of treated cells - Optical density DMSO) / (Optical density of control cells - Optical density DMSO)] x 100.

Half-inhibitory concentrations (IC_{50}) represent the concentrations of the tested samples required to inhibit 50% cell proliferation (compared to the solvent control, which showed no differences in comparison to untreated control) and were calculated from the mean values of data from wells.

2.4. Cell-cycle analysis

Changes in cell-cycle distribution were assessed by flow cytometry. HCT116 cells in complete growth medium at a density of 2 x 10^5 cells/well were seeded in 12-well plates (final volume 1 mL). After 24 h, the cells were treated with **1** (0.2 - 0.8 µM) for 24, 48 and 72 h. Cells treated with DOX 0.6 µM or HU 2 mM, both compounds dissolved in sterile water, were simultaneously run as positive controls. Control cells were devoid of **1**, containing only 1% acetonitrile. After treatment, cells were collected and fixed in 70% ice-cold ethanol and kept at -20°C for at least 24 h. Before analysis, the cells were washed twice and suspended in a solution of PBS containing 50 µg/mL PI and 100 µg/mL RNase A and incubated for 30 min at room temperature in the dark. Cellular DNA content was analyzed by flow cytometry. The relative distribution of at least 10,000 cells was analyzed using FlowJo software version 7.6.2 (Tree Star, Inc. Ashland, OR).

2.5. 5-bromo-2'-deoxyuridine incorporation assay

HCT116 cells in complete growth medium at a density of 5 x 10^5 cells/well were seeded in 6-well plates (final volume 2 mL). After a 24 h period, cells were treated with **1** (0.2 - 0.8 µM) for 24, 48 and 72 h. Control cells were devoid of **1**, containing only 1% acetonitrile. Cells treated with HU 2 mM dissolved in sterile water were simultaneously run. For detection of replicative DNA synthesis, 10 µM BrdU was added 20 min before collecting the cells. Cells were fixed in 70% ice-cold ethanol, permeabilized with 2N HCl and 0.5% TritonX-100 for 15 min at room temperature and neutralized with sodium borate 0.1 M (pH 8.5). After washing twice with PBSTB (PBS, Tween 0.2% and BSA 0.5%), cells were incubated with 100 µL of anti-BrdU antibody, clone BU-1 from Millipore, for 1h at room temperature. Subsequently, cells were washed twice with PBSTB, spun down and incubated for 1 h with a FITC-conjugated secondary antibody from Jackson ImmunoResearch. After labeling, cells were washed as described above and re-suspended in PBS containing PI (50 µg/mL) and RNase A (100 µg/mL), and incubated for 30 min at room temperature in the dark. Samples were immediately analyzed by flow cytometry. The relative distribution of at least 10,000 cells was analyzed using FlowJo software version 7.6.2 (Tree Star, Inc. Ashland, OR).

2.6. SYTOX Red dead cell stain

HCT116 cells in complete growth medium were seeded at a density of 2 x 10^5 cells/well in 12-well plates (final volume 1 mL). After 24 h, cells were treated with **1** (0.2 - 0.8 µM), DOX 0.6 µM or HU 2 mM during 24, 48 and 72 h. Control cells containing 1% acetonitrile were simultaneously run. After treatment, cells were harvested and stained with 5 nM of SYTOX Red stain, following the manufacturer's protocol. Samples were analyzed by flow cytometry. The relative distribution of at least

10,000 cells was analyzed using FlowJo software version 7.6.2 (Tree Star, Inc. Ashland, OR).

2.7. Assessment of apoptosis by Annexin V/SYTOX Red double staining assay

HCT116 cells (2 x 10^5/well) cultured in complete growth medium were plated in 12-well plates (final volume 1 mL) for 24 h and then treated with compound **1** 0.2 µM, HU 2 mM or 1% acetonitrile for 24, 48 and 72 h. After incubation, cells were harvested, washed and suspended in cold PBS. The proportion of cells undergoing apoptosis was examined by a double staining experiment using a FITC labeled Annexin V and SYTOX Red, as instructed by the manufacturer´s protocol. At least 10,000 cells were analyzed and quadrant analysis was performed using FlowJo software version 7.6.2 (Tree Star, Inc. Ashland, OR). Cells in early stages of apoptosis stained as Annexin V^+/SYTOX Red $^-$, whereas cells in late apoptosis stained as Annexin V^+/SYTOX Red^+.

2.8. Colony formation assay

HCT116 cells were seeded in 96-well plates at a density of 2 x 10^4 cells/well. After 24 h, cells were treated with **1** (0.02 µM – 0.4 µM) or 1% acetonitrile for 72 h. To evaluate the remnant ability of a single cell to grow into a colony after treatment, cells were harvested, counted and immediately re-plated in 6-well plates containing drug-free medium at different densities ranging from 80-2560 cells per well. After 10 days of incubation, colonies were washed with PBS, fixed and stained with a mixture of MeOH / glacial acetic acid 75:25 containing 0.5% crystal violet for 30 min at room temperature. After staining, plates were carefully washed by immersion in tap water and

left to dry. Colonies were counted using ImageJ software. Plating efficiency (PE) of control cells was calculated as PE = (number of colonies formed/number of cells seeded). The percentage surviving fraction (SF%) after treatments was calculated in terms of PE as follows: SF = [number of colonies formed after treatment/(number of cells seeded x PE)] x 100.

2.9. Western Blot

HCT116 cells (5 x 10^5 cells/well) were seeded in 6-well plates containing complete growth medium, cultured for 24 h and then treated with **1** (0.2-0.8 µM), DOX 0.6 µM, HU 2 mM or 1% acetonitrile during 24 and 48 h (final volume 2 mL). After treatment, samples were lysed directly in Laemmli buffer. Western blots were performed using anti-p21 antibody (C19- Santa Cruz, USA), polyclonal antibody against human p53 (1801- Santa Cruz, USA) and a polyclonal antibody against actin as a loading control (Sigma-Aldrich CO,St Louis, MO). Secondary antibodies coupled to infrared dyes were used for detection using an Odyssey® CLx Imaging System (LI-COR Corporate, USA). Data analysis and quantifications for each protein, correcting for loading, was performed using Image Studio software (LI-COR Corporate, USA).

2.10. Effect on the isogenic cell lines HCT116 p53 $^{-/-}$ and HCT116 p21$^{-/-}$

To determine if the induction of p21 and p53 was actively implicated in the cytotoxicity induced by **1**, the effect of this was evaluated in a co-culture of wild-type HCT116 and its isogenic derivatives HCT116 p53 $^{-/-}$ and HCT116 p21 $^{-/-}$ tagged with different fluorescent proteins. Briefly, three isogenic cell lines were cultured separately

and, 24 h prior to the addition of **1** (0.01 – 0.2 μM) or 1% acetonitrile, they were co-plated in equal numbers in a multi-well plate. A mixture of isogenic cell lines (4,000 cells per 96-well) was cultured for 6 days and the differential survival was assessed by analyzing the ratio of the different cell populations by FACS analysis. The similar proliferation index of each cell line without treatment was confirmed in the control group corresponding to each experiment.

2.11. Statistical analysis

The results are expressed as mean ± SE. Data were analyzed using two-way analysis of variance (ANOVA) using GraphPad Prism software (GraphPad Prism 5.0, GraphPad Software, Inc., CA, USA), with p -values ≤ 0.05 as statistically significant. All experiments were conducted in duplicate or triplicate at least three times in independent experiments. The 50% inhibitory concentrations (IC_{50}) were calculated by log-probit analysis, responding to at least ten concentrations at the 95% confidence level with upper and lower confidence limits.

3. Results

*3.1 Compound **1** exerted a potent and selective cytotoxic effect against HCT116 cells*

The anti-proliferative effect of **1** was evaluated by MTT assay against a panel of tumor-derived cell lines. Compound **1** showed a strong cytotoxic effect against all the cell lines evaluated, with IC_{50} values ranging from 0.2 to 4.6 μM (Table 1). The IC_{50} values were in all cases below 10 μM, the threshold established by the US National

Cancer Institute plant screening program for considering a pure compound as cytotoxic (Kuete et al., 2014). This activity was considerably stronger in HCT116 cells, with an IC_{50} value of 0.2 μM. The half-inhibitory effect of **1** was in a similar range to that found for DOX (IC_{50} = 0.1-5.1 μM), which was used as a positive control.

Based on these findings, the HCT116 cell line was selected for subsequent studies to examine the molecular mechanisms underlying the antitumoral effect mediated by **1**.

*3.2. Compound **1** induced S phase cell cycle arrest*

After treatment with cytotoxic agents, cells can enter into a death program or stop their cell cycle progression, which in turn can also trigger death by apoptosis if cells cannot overcome the damage (León et al., 2009). To assess the influence of **1** on the progression of HCT116 cells through the cell cycle, the DNA content after PI staining was analyzed. Intriguingly, treatment with **1** led to a time-dependent increase (b = 0.011; p = 0.0029; CI 95% = 0.004-0.017) in the number of cells transiting the S-phase of the cell cycle (Fig. 2). After 24 h of treatment with **1**, the cells began to accumulate in the S-phase (Fig. 2A and B). This effect became significant ($p < 0.001$) after 48 h, leading to percentages of S-phase cells up to 2 times higher than in control cells (Fig. 2B). This arrest remained even after 72 h of exposure to **1** at 0.4 and 0.8 μM ($p < 0.001$) (Fig. 2B). In addition to DOX, which is known to induce G2-M arrest (Rezaei et al., 2012), HU was introduced as a second positive control, since it is well-established that it induces accumulation of S-phase cells by ribonucleotide deprivation (Gottifredi et al., 2001a). Remarkably, while HU triggered the accumulation of cells at the G1-S transition, **1** induced the accumulation of cells throughout S-phase (Fig. 2A).

No significant differences ($p > 0.05$) were observed between the absolute number of cells in S-phase between this positive control and compound **1** at 0.4 and 0.8 µM at 48 and 72 h of treatment (Fig. 2B).

To gain further insight in the type of S-phase arrest induced by **1,** BrdU (5-bromo-2'-deoxyuridine) incorporation experiments were performed. BrdU is a thymidine analogue that incorporates into newly synthesized DNA. This type of experiment enables cell cycle arrest to be determined and also whether the S/phase accumulation is linked to a delay in the progression through S-phase or to a permanent block within this phase (by the evaluation of the percentage of cells actively synthesizing DNA, $BrdU^+$ vs $BrdU^-$). In agreement with the results obtained when analyzing DNA content after PI staining alone (Fig. 2A), a strong arrest was observed at the G1/S transition after HU treatment and a widespread arrest after treatment with **1** in S-phase at 48 and 72 h (Fig. 3A). Subsequently, the percentage of $BrdU^+$ vs $BrdU^-$ within S-phase at different time points after treatment was quantified. While at 24 h the results were consistent with a delay in S-phase progression, at 48 and mainly at 72 h it became evident that a sub-population of cells treated with **1** were no longer incorporating BrdU (Fig. 3B), and therefore could be considered as permanently arrested.

*3.3. Compound **1** triggered cell death in a time-dependent manner*

Since it is well-established that a permanent arrest in S-phase is an event that would eventually lead to cell death (Gottifredi and Prives, 2005), we decided to further explore this effect with **1**. In fact, the experiments of PI incorporation (Fig. 2A) showed that the accumulation of cells in S-phase was accompanied by an increase in the hypo-

diploid (sub-G1) population after 48 h of treatment with **1**, suggesting the concomitant induction of cell death. To confirm this, cell death induction was assessed by flow cytometry using SYTOX Red stain. It was observed that **1** induced cell death in HCT116 cells in a time-dependent manner (b = - 0.825; p = < 0.0001; CI 95% = -0.984 to -0.666) (Fig. 4A). While the percentage of viable cells in DOX treatment differed with respect to control only at 72 h (p < 0.001), HU showed significant differences (p < 0.001) from 48 h and the treatments with **1** showed significant differences (p < 0.001) at all assayed times from 0.2 μM (Fig. 4A). On the other hand, after 72 h, treatment with **1** at 0.2, 0.4 and 0.8 μM showed a 53%, 64% and 66% death, respectively (Fig. 4B).

*3.4. Compound **1** led to apoptotic cell death and reduced the proliferative potential of HCT116 cells*

The experiments using SYTOX Red stain enabled confirmation of the induction of cell death when **1** was applied at the dose of 0.2 μM. Since many anticancer drugs, including those from natural origin, exert their effect through different mechanisms that ultimately trigger apoptotic cell death (Pieme et al., 2014), we examined whether the cell death observed was in fact apoptosis. After treatment, HCT116 cells were double-stained using Annexin V-FITC and SYTOX Red to discriminate between apoptosis and other types of death such as necrosis (Liao and Lieu, 2005). Data analysis showed an increase in the proportion of cells undergoing apoptosis, with 74.3% of early and late apoptotic cells after 72 h exposure to **1** (Fig. 5). It is worth noting that a small percentage of necrotic cells (SYTOX Red $^{+}$ / Annexin V-FITC $^{-}$) were observed at 24 h of treatment with **1**, which suggests that apoptosis may be the main, but not the only mechanism involved (Fig. 5).

Another important question for exploring the potential of compound **1** as a potent antitumoral agent was the proliferative capacity of the small percentage of cells that survive the treatment. To evaluate this, a clonogenic assay was carried out (Franken et al., 2006). After being submitted to different concentrations of **1** for 72 h of treatment, HCT116 cells were re-plated at a very low density in drug-free growth medium to evaluate the remnant capacity of individual cells to generate colonies. We found that **1** remarkably reduced the clonogenic capacity of HCT116 cells, with a mean survival fraction of 0.04 µM (Fig. 6A), which is five times lower than the IC_{50} determined by the MTT assay (0.2 µM).

*3.5. The antitumoral activity of **1** was dependent on p53*

As previously stated, compound **1** induced S-phase cell cycle arrest and apoptosis in HCT116 cells. Considering the key role of p53 and p21 in the cellular response against genotoxic agents (Gottifredi et al., 2001a; Mansilla et al., 2013), the goal of this study was to evaluate the effect of **1** on the expression of both proteins. It was found that treatment with **1** (0.2-0.8 µM) increased the expression of p53 and p21 proteins in a time- and dose-dependent manner (Fig. 7A). The expression profile of these proteins was similar to the treatment with HU but not to that with DOX (Fig. 7A).

To determine if the induction of p21 and p53 is actively implicated in the cytotoxicity induced by **1**, an assay was performed to assess in parallel the cell survival in a co-culture condition of HCT116 wild-type cells with two isogenic derivatives (HCT116 $p53^{-/-}$ and $p21^{-/-}$). In this assay, each cell line was recognized by the stable expression of fluorescent proteins. When the effect of **1** was evaluated using this assay, an outstanding differential sensitivity was found of $p53^{-/-}$ cells in comparison to $p21^{-/-}$

and wild-type cells (Fig. 7B). Indeed, at 0.2 μM, more than 80% of the viable cells corresponded to $p53^{-/-}$. We concluded that the expression of p53 (but not of p21) is critical for the cytotoxicity exerted by **1**.

4. Discussion

The fact that cancer still has high mortality rates encourages researchers to find novel candidate compounds for therapies. With this in mind, the cytotoxic effect of an isomeric mixture (**1**) formed by two interchangeable tetranortriterpenoids, meliartenin and 12-hydroxyamoorastatin (Fig. 1) (Carpinella et al., 2002), was evaluated against a panel of tumor cell lines. As observed in Table 1, compound **1** showed a strong cytotoxic activity (0.2 - 4.6 μM) on CCRF-CEM, K562, A549 and HCT116 cells. Comparing the inhibitory values among the assayed cell lines, it was noteworthy that **1** exerted a highly specific toxic effect against HCT116. This was evident from the IC_{50} ratios calculated. In fact, when the IC_{50} values of **1** against CCRF-CEM (IC_{50} = 1.4 μM), K562 (IC_{50} = 4.6 μM) and A549 (IC_{50} = 4.3 μM) were compared to those of HCT116 cells (IC_{50} = 0.2 μM), ratios of 7, 23 and 22 were observed, respectively. Taking into account previous classifications, IC_{50} ratios higher than 6 are rated as highly selective (Acton et al., 1994). In contrast, this specificity with respect to all the assayed cells was not observed with the commercial chemotherapeutic agent DOX, which was used as a positive control (Table 1).

Our first intriguing finding was that treatment with **1** induced a time-dependent increase in the number of cells transiting the S-phase of the cell cycle, with a similar activity from 0.4 μM to that obtained with HU at 48 and 72 h (Fig. 2B). Subsequent detection with an anti-BrdU antibody confirmed a sustained anti-proliferative effect of **1**

on HCT116 cells (Fig. 3A and B). This is remarkable considering that compounds shown to induce arrest at the S-phase are quite rare (Hu et al., 2007). S-phase-arresting natural products, many of them derived from plants, have been evaluated for their potential clinical utility. Among these, β-lapachone, an ortho naphthoquinone originally isolated from the tree *Tabebuia avellanedae* (commonly known as Lapacho) (Pardee et al., 2002), is currently undergoing Phase I clinical trials against solid tumors (Cheriyamundath et al., 2017). Interest in such compounds relies on the fact that DNA replication is a critical process that can be delayed, but cannot be indefinably arrested (Gottifredi and Prives, 2005), thus turning S-phase into a "strategic" stage for targeting tumor cells. A good example is the case of HU, a S-phase arresting agent that has had great success in the treatment of several types of blood cancers (Leitch et al., 2016). Our data demonstrated that, similar to HU, the stronger induction of cell death correlates with the time points at which the arrest of S-phase becomes permanent (Fig. 3B and Fig. 5).

In addition to slowing down the cellular progression through S-phase, flow cytometry analysis after SYTOX Red stain showed that **1** induced cell death in a time-dependent manner (Fig. 4A), reaching percentages of death higher than 53% from 0.2 μM at 72 h (Fig. 4B). These results indicated that cells could not overcome the S-phase arrest induced by this compound, leading to cell death. Moreover, this percentage of cell death observed after 72 h of treatment with **1** at 0.2 μM was consistent with the IC_{50} determined by MTT (IC_{50} = 0.2 μM, Table 1), indicating that the anti-proliferative effect observed after treatment with **1** is a consequence of cell death rather than of a permanent arrest of the cell cycle.

Furthermore, Annexin V/SYTOX Red double staining demonstrated that **1** was able to induce apoptosis in HCT116 cells (Fig. 5) with values higher than 70% at 72 h.

Thus, our results suggest that **1** triggers apoptosis due to a sustained blockage of S-phase progression.

It was also found that **1** was not only capable of killing HCT116 but also strongly impaired its clonogenic potential at a concentration as low as 0.04 μM (Fig. 6), which reinforces its potential as an effective antitumor agent. This is a very important finding, since drugs that suppress clonogenicity hold potential to treat a variety of tumors by inhibiting their ability to expand and colonize (Cheriyamundath et al., 2017).

Few studies have been reported regarding the mechanism of cytotoxicity exerted by limonoids isolated from *M. azedarach.* 12-O-acetylazedarachin B (Zhou et al., 2016), toosendanin, meliarachin C and 3-O-deacetyl-4'-demethyl-28-oxosalaninin (Akihisa et al., 2013) were found to exert antiproliferative and apoptotic effects on HL-60 cells (Akihisa et al., 2013; Ju et al., 2013; Zhou et al., 2016). Particularly, 12-O-acetylazedarachin B, meliarachin C and toosendanin, all of them trichilin-type limonoids like meliartenin and 12-hydroxyamoorastatin, presented lower IC_{50} values (0.016, 0.65 and 0.005 μM, respectively by MTT assay) over HL60 cells compared to those obtained for the salannin-type limonoid 3-O-deacetyl-4'-demethyl-28-oxosalaninin (IC_{50} = 2.8 μM by MTT assay). Takeya et al. evaluated some azadirachtin- and trichilin-type limonoids against P388 lymphocytic leukemia cells, and the latter showed the lowest inhibitory values (Takeya et al., 1996a; 1996b). This improved cytotoxic activity observed for trichilin-type limonoids may be related to some characteristic structural features that merit further consideration. Most trichilin-type limonoids contain both a C-19/28 oxygen bridge and a C14/15-epoxide ring, which were found to be involved in cell growth inhibition (Tan and Luo, 2011). The comparison of the IC_{50} values of 12-hydroxyamoorastatin (0.004 μM) and the C14/15 epoxy lacking amoorastatone (58 μM), both compounds isolated from *Aphanamixis*

grandifolia (Meliaceae), against P388 lymphocytic leukemia cells suggest that this group is required for improved cytotoxic activity (Polonsky et al., 1979). Similarly, toosendanin isolated from *Melia toosendan* (Meliaceae), which also contains the C14/15 epoxide, resulted highly cytotoxic against KB cells, whereas toosendanal, obtained from the same tree and possessing a C-15 keto structure, was not toxic to the same cells (Tada et al., 1999).

In the light of our findings and considering the key role of p53 in the integration of signals from diverse pathways that regulate the cell cycle and apoptosis (Finlan and Hupp, 2005; Maddika et al., 2007), we evaluated whether the biological effects mediated by **1** were related to the induction and activity of p53 and its downstream target p21. The increased expression profile of these proteins was similar to treatment with HU but not with DOX (Fig. 7A). This is consistent with previous findings, showing that HU induced an arrest in S-phase, where the induction of p53 and p21 is known to be subtle (Gottifredi et al., 2001a). In contrast, treatment with DOX triggered a stronger induction of p53 and p21 (Fig. 7A), which correlates with a robust cell cycle arrest in G2 (Fig. 2A).

It was found that p53-dependent apoptosis was responsible for the cytotoxicity observed in HCT116 after treatment with **1** (Fig. 7A and B). The fact that p53, but not p21, was linked to the cytotoxic effect mediated by **1** strongly suggests that only the pro-apoptotic functions of p53 are critical for this effect. In fact, while it is well-established that the p53/p21 axis promotes cell cycle arrest in G1 and G2, p21 is actively maintained at low levels by transcriptional and proteolytic mechanisms during the S-phase (Soria and Gottifredi, 2010). This might explain the attenuated accumulation of p21 induced by **1** in comparison to DOX (Fig 7A). Moreover, an analogous interpretation could be drawn in relation to the similar sensitivity observed in

$p21^{-/-}$ cells versus parental HCT116 cells (Fig 7B), because both cell lines share a wt p53 status. The requirement of a normal expression of p53 to trigger an efficient execution of the death program (Lowe et al., 1993) could explain, at least in part, the different results obtained in inhibitory values between the colorectal carcinoma cells HCT116 and both leukemia cell lines, CCRF-CEM and K562.

As previously stated, although compound **1** was considered effective for inhibiting both leukemic cell lines (IC_{50} = 1.4 and 4.6 μM, for CCRF-CEM and K562, respectively), it proved remarkably more effective for inducing death over the HCT116 cells (IC_{50} = 0.2 μM). Beyond the different genetic backgrounds among these cell lines, it is important to highlight that both leukemia-derived cell lines are p53-mutated, in contrast to HCT116. Briefly, sequencing of the p53 gene in the K562 cell line demonstrated a mutation in exon 5, characterized by a single base insertion (cytosine) between codons 135 and 136 (Law et al., 1993). This frameshift mutation leads to an N-terminal truncated protein of 147 amino acids. Only the mutated sequence was present, suggesting that the normal allele has been lost. On the other hand, CCRF-CEM cells are also p53-mutated in codons 524 and 743, but these cells are heterozygous for this mutation (Geley et al., 1997). This heterozygosity of CCRF-CEM cells could explain their higher sensitivity to **1** (IC_{50} = 1.4 μM) than to K562 (IC_{50} = 4.6 μM). A similar approach could be applied to explain the results found in studies performed with other cell lines exposed to 12-hydroxyamoorastatin. Comparing the IC_{50} values obtained for the tumor cell lines SK-OV-3, HCT-15, A549; XF-498 and SK-MEL-2 (Ahn et al., 1994) with their p53 status, a possible explanation could be drawn. From the IC_{50} values reported by Ahn et al. (Ahn et al., 1994), the SK-OV-3 was the least sensitive to the treatment. This cell line carries a homozygous mutation for p53 (C.267delC), while the most affected cell lines are heterozygous (HCT-15 and SK-MEL-2) or wild-type (A549

and XF-498). It is worth mentioning that, despite A549 cells being p53 wt, this cell line was not the most affected. This could be explained by the fact that these cells are characterized by a stable over-expression of the Nrf2 transcription factor, which is involved in the promotion of a cellular protective response against different toxic aggressions (Wang et al., 2008). Indeed, these cells have shown enhanced resistance to a broad spectrum of chemotherapeutic agents, including cisplatin, DOX and etoposide (Wang et al., 2008). This is in accordance with the lower sensitivity that these cells showed when treated with DOX or compound **1** in our experiments.

Taken together, the results described in this work position compound **1** as a strong antitumoral agent, with great potential for targeting $p53^{+}$ tumors. The present investigation is the first effort toward a comprehensive understanding of the mechanisms underlying the anticancer activity of compound **1**. This information is of great value for positioning **1** as a promising antitumor agent that may be used to improve anticancer therapy.

Acknowledgments

We thank Joss Heywood for revising the English language. M.B. Joray, S.M. Palacios, J.L. Bocco, G. Soria and M.C. Carpinella, are staff members of the National Research Council of Argentina (CONICET). This research project was conducted with the support from Catholic University of Córdoba, MINCyT Córdoba (GRF 2008, PID 2012) CONICET (PIP 11220100100236), PICT 2014-1594 and PICT Start-up 2013-1553. MLG, MIC and JL acknowledge receipt of a Scholarship from CONICET.

Conflict of interest

The authors declare that there are no conflicts of interest.

References

Acton, E.M., Narayanan, V.L., Risbood, P.A., Shoemaker, R.H., Vistica, D.T., Boyd, M.R., 1994. Anticancer specificity of some ellipticinium salts against human brain tumors in vitro. J. Med. Chem. 37, 2185–2189.

Ahn, J.-W., Choi, S.-U., Lee, C.-O., 1994. Cytotoxic limonoids from Melia azedarach var. Japonica. Phytochemistry 36, 1493–1496.

Ahn, J.-W., Yoo, G.-S., No, Z., Lee, S.-H., 1993. 12-Hydroxyamoorastatone, a New Limonoid from Melia azedarach var. Japonica. Bulletin of the Korean Chemical Society 14, 554–556.

Akihisa, T., Pan, X., Nakamura, Y., Kikuchi, T., Takahashi, N., Matsumoto, M., Ogihara, E., Fukatsu, M., Koike, K., Tokuda, H., 2013. Limonoids from the fruits of Melia azedarach and their cytotoxic activities. Phytochemistry 89, 59–70.

Balunas, M.J., Kinghorn, A.D., 2005. Drug discovery from medicinal plants. Life Sci. 78, 431–441.

Brown, C.J., Lain, S., Verma, C.S., Fersht, A.R., Lane, D.P., 2009. Awakening guardian angels: drugging the p53 pathway. Nat Rev Cancer 9, 862–873.

Bunz, F., Dutriaux, A., Lengauer, C., Waldman, T., Zhou, S., Brown, J.P., Sedivy, J.M., Kinzler, K.W., Vogelstein, B., 1998. Requirement for p53 and p21 to sustain G2 arrest after DNA damage. Science 282, 1497–1501.

Carpinella, M.C., Ferrayoli, C., Valladares, G., Defago, M., Palacios, S., 2002. Potent limonoid insect antifeedant from Melia azedarach. Biosci. Biotechnol. Biochem. 66, 1731–1736.

Cheriyamundath, S., Mahaddalkar, T., Kantevari, S., Lopus, M., 2017. Induction of acetylation and bundling of cellular microtubules by 9-(4-vinylphenyl) noscapine elicits S-phase arrest in MDA-MB-231 cells. Biomed. Pharmacother. 86, 74–80.

Efferth, T., Davey, M., Olbrich, A., Rücker, G., Gebhart, E., Davey, R., 2002. Activity of drugs from traditional Chinese medicine toward sensitive and MDR1- or MRP1-overexpressing multidrug-resistant human CCRF-CEM leukemia cells. Blood Cells Mol. Dis. 28, 160–168.

Ferlay, J., Soerjomataram, I., Dikshit, R., Eser, S., Mathers, C., Rebelo, M., Parkin, D.M., Forman, D., Bray, F., 2015. Cancer incidence and mortality worldwide: sources, methods and major patterns in GLOBOCAN 2012. Int. J. Cancer 136, E359–86.

Finlan, L.E., Hupp, T.R., 2005. The Life Cycle of P53: A Key Target in Drug Development, in: Apoptotic Pathways as Targets for Novel Therapies in Cancer and Other Diseases. Springer-Verlag, New York, pp. 157–172.

Foster, I., 2008. Cancer: A cell cycle defect. Radiography 14, 144–149.

Franken, N.A.P., Rodermond, H.M., Stap, J., Haveman, J., van Bree, C., 2006. Clonogenic assay of cells in vitro. Nat Protoc 1, 2315–2319.

Geley, S., Hartmann, B.L., Hattmannstorfer, R., Löffler, M., Ausserlechner, M.J., Bernhard, D., Sgonc, R., Strasser-Wozak, E.M., Ebner, M., Auer, B., Kofler, R., 1997. p53-induced apoptosis in the human T-ALL cell line CCRF-CEM. Oncogene 15, 2429–2437.

Gottifredi, V., Prives, C., 2005. The S phase checkpoint: when the crowd meets at the fork. Semin. Cell Dev. Biol. 16, 355–368. doi:10.1016/j.semcdb.2005.02.011

Gottifredi, V., Shieh, S., Taya, Y., Prives, C., 2001a. p53 accumulates but is functionally impaired when DNA synthesis is blocked. Proc. Natl. Acad. Sci. U.S.A. 98, 1036–1041.

Gottifredi, V., Shieh, S., Taya, Y., Prives, C., 2001b. p53 accumulates but is functionally impaired when DNA synthesis is blocked. Proc. Natl. Acad. Sci.

U.S.A. 98, 1036–1041.

Hu, L., Li, Z.-R., Li, J.-N., Qu, J., Jiang, J.-D., Boykin, D.W., 2007. 3-(2'-Bromopropionylamino)-benzamides as novel S-phase arrest agents. Bioorg. Med. Chem. Lett. 17, 6847–6852.

Itokawa, H., Qiao, Z.S., Hirobe, C., Takeya, K., 1995. Cytotoxic limonoids and tetranortriterpenoids from Melia azedarach. Chem. Pharm. Bull. 43, 1171–1175.

Joray, M.B., Trucco, L.D., González, M.L., Napal, G.N.D., Palacios, S.M., Bocco, J.L., Carpinella, M.C., 2015. Antibacterial and Cytotoxic Activity of Compounds Isolated from Flourensia oolepis. Evid Based Complement Alternat Med 2015, 912484–11.

Ju, J., Qi, Z., Cai, X., Cao, P., Liu, N., Wang, S., Chen, Y., 2013. Toosendanin induces apoptosis through suppression of JNK signaling pathway in HL-60 cells. Toxicol In Vitro 27, 232–238.

Kristanc, L., Kreft, S., 2016. European medicinal and edible plants associated with subacute and chronic toxicity part I: Plants with carcinogenic, teratogenic and endocrine-disrupting effects. Food Chem. Toxicol. 92, 150–164.

Kuete, V., Ango, P.Y., Yeboah, S.O., Mbaveng, A.T., Mapitse, R., Kapche, G.D.W.F., Ngadjui, B.T., Efferth, T., 2014. Cytotoxicity of four Aframomum species (A. arundinaceum, A. alboviolaceum, A. kayserianum and A. polyanthum) towards multi-factorial drug resistant cancer cell lines. BMC Complementary and Alternative Medicine 2014 14:1 14, 340.

Law, J.C., Ritke, M.K., Yalowich, J.C., Leder, G.H., Ferrell, R.E., 1993. Mutational inactivation of the p53 gene in the human erythroid leukemic K562 cell line. Leukemia Research 17, 1045–1050.

Leitch, C., Osdal, T., Andresen, V., Molland, M., Kristiansen, S., Nguyen, X.N.,

Bruserud, Ø., Gjertsen, B.T., McCormack, E., 2016. Hydroxyurea synergizes with valproic acid in wild-type p53 acute myeloid leukaemia. Oncotarget 7, 8105–8118.

León, L.G., Donadel, O.J., Tonn, C.E., Padrón, J.M., 2009. Tessaric acid derivatives induce G2/M cell cycle arrest in human solid tumor cell lines. Bioorg. Med. Chem. 17, 6251–6256.

Liao, P.-C., Lieu, C.-H., 2005. Cell cycle specific induction of apoptosis and necrosis by paclitaxel in the leukemic U937 cells. Life Sci. 76, 1623–1639.

Lowe, S.W., Ruley, H.E., Jacks, T., Housman, D.E., 1993. p53-dependent apoptosis modulates the cytotoxicity of anticancer agents. Cell 74, 957–967.

Maddika, S., Ande, S., Panigrahi, S., Paranjothy, T., Weglarczyk, K., Zuse, A., Eshraghi, M., Manda, K., Wiechec, E., Los, M., 2007. Cell survival, cell death and cell cycle pathways are interconnected: Implications for cancer therapy. Drug Resistance Updates 10, 13–29.

Mansilla, S.F., Soria, G., Vallerga, M.B., Habif, M., Martínez-López, W., Prives, C., Gottifredi, V., 2013. UV-triggered p21 degradation facilitates damaged-DNA replication and preserves genomic stability. Nucleic Acids Res. 41, 6942–6951.

Mirzayans, R., Andrais, B., Scott, A., Murray, D., 2012. New insights into p53 signaling and cancer cell response to DNA damage: implications for cancer therapy. J. Biomed. Biotechnol. 2012, 170325.

Pardee, A.B., Li, Y.Z., Li, C.J., 2002. Cancer therapy with beta-lapachone. Curr Cancer Drug Targets 2, 227–242.

Pieme, C.A., Kumar, S.G., Dongmo, M.S., Moukette, B.M., Boyoum, F.F., Ngogang, J.Y., Saxena, A.K., 2014. Antiproliferative activity and induction of apoptosis by Annona muricata (Annonaceae) extract on human cancer cells. BMC Complementary and Alternative Medicine 2014 14:1 14, 1.

Polonsky, J., Varon, Z., Marazano, C., Arnoux, B., Pettit, G.R., Schmid, J.M., Ochi, M., Kotsuki, H., 1979. The structure of amoorastatone and the cytotoxic limonoid 12-hydroxyamoorastatin. Experientia 35, 987–989.

Rezaei, P.F., Fouladdel, S., Hassani, S., Yousefbeyk, F., Ghaffari, S.M., Amin, G., Azizi, E., 2012. Induction of apoptosis and cell cycle arrest by pericarp polyphenol-rich extract of Baneh in human colon carcinoma HT29 cells. Food Chem. Toxicol. 50, 1054–1059.

Rumjanek, V.M., Vidal, R.S., Maia, R.C., 2013. Multidrug resistance in chronic myeloid leukaemia: how much can we learn from MDR-CML cell lines? Biosci. Rep. 33, 875–888.

Soria, G., Gottifredi, V., 2010. PCNA-coupled p21 degradation after DNA damage: The exception that confirms the rule? DNA Repair (Amst.) 9, 358–364.

Tada, K., Takido, M., Kitanaka, S., 1999. Limonoids from fruit of Melia toosendan and their cytotoxic activity. Phytochemistry 51, 787–791.

Takeya, K., Qiao, Z.S., Hirobe, C., Itokawa, H., 1996a. Cytotoxic azadirachtin-type limonoids from Melia azedarach. Phytochemistry 42, 709–712.

Takeya, K., Quio, Z.S., Hirobe, C., Itokawa, H., 1996b. Cytotoxic trichilin-type limonoids from Melia azedarach. Bioorg. Med. Chem. 4, 1355–1359.

Tan, Q.-G., Luo, X.-D., 2011. Meliaceous limonoids: chemistry and biological activities. Chem. Rev. 111, 7437–7522.

Waldman, T., Kinzler, K.W., Vogelstein, B., 1995. p21 is necessary for the p53-mediated G1 arrest in human cancer cells. Cancer Res. 55, 5187–5190.

Wang, X.-J., Sun, Z., Villeneuve, N.F., Zhang, S., Zhao, F., Li, Y., Chen, W., Yi, X., Zheng, W., Wondrak, G.T., Wong, P.K., Zhang, D.D., 2008. Nrf2 enhances resistance of cancer cells to chemotherapeutic drugs, the dark side of Nrf2.

Carcinogenesis 29, 1235–1243.

Zhao, L., Huo, C.-H., Shen, L.-R., Yang, Y., Zhang, Q., Shi, Q.-W., 2010. Chemical constituents of plants from the genus Melia. Chemistry & biodiversity 7, 839–859.

Zhou, F., Ma, X.-H., Li, Z.-J., Li, W., Zheng, W.-M., Wang, Z.-B., Zeng, X.-M., Sun, K.-H., Zhang, Y.-H., 2016. Four New Tirucallane Triterpenoids from the Fruits of Melia azedarach and Their Cytotoxic Activities. Chem. Biodivers. 13, 1738–1746.

Legends for figures

Fig. 1. Chemical structures of the constituents of the isomeric mixture of tetranortriterpenoids (**1**) meliartenin (A) and 12-hydroxyamoorastatin (B).

Fig. 2. Treatment with **1** triggered S-phase accumulation A) HCT116 cells were plated in 12-well plates and, 24 h later, the cells were treated with **1** at 0.2, 0.4 and 0.8 µM, 1% acetonitrile (control), doxorubicin (DOX) 0.6 µM or hydroxyurea (HU) 2 mM. After a 24, 48 and 72 h incubation period, cells were fixed and stained with propidium iodide (PI). DNA content was analyzed by flow cytometry. Histograms are representative of three independent experiments. B) The cell cycle profiles obtained in A) were analyzed using Flowjo and the percentage of cells at each phase of the cell cycle was quantified. Data are presented as mean ± SE of three independent experiments. Differences with respect to control were analyzed using two-way analysis of variance (ANOVA) (*** $p < 0.001$, ** $p < 0.01$).

Fig. 3. S-phase progression is permanently blocked after treatment with **1** A) HCT116 cells were treated with **1** at 0.2, 0.4 and 0.8 µM and HU for 24, 48 and 72 h. After exposure, cells were pulsed for 20 min with BrdU and immediately fixed with 70% ice-cold ethanol at 4°C. Subsequently, cells were stained with propidium iodide (PI) and processed for BrdU detection, using a specific antibody followed by a secondary antibody conjugated to FITC. Dual channel flow cytometry was performed to determine the DNA content and BrdU simultaneously. A representative plot of three independent

experiments at 0.2 μM is shown. B) The percentage of $BrdU^+$ vs $BrdU^-$ cells within the S-phase at different time points was calculated using Flowjo.

Fig. 4. Treatment with **1** triggered cell death in a time-dependent manner A) HCT116 cells were plated in 12-well plates and 24 h later were treated with **1** at 0.2, 0.4 and 0.8 μM, 1% acetonitrile (control), doxorubicin (DOX) 0.6 μM or hydroxyurea (HU), 2 mM for a period of 24, 48 and 72 h. After treatment, cells were collected and stained with SYTOX Red dead cell stain and analyzed by flow cytometry. Viable cells ($Sytox\ Red^-$) can be distinguished from dead cells ($SYTOX\ Red^+$). Data are represented as the mean ± SE of three independent experiments. Histograms are representative of three independent experiments. B) Representative profile of SYTOX Red dead cell stain at 72 h post treatment with **1**, HU and DOX.

Fig. 5. Treatment with **1** triggers apoptosis. HCT116 cells were plated in 12-well plates and 24 h later were treated with **1** at 0.2 μM, 1% acetonitrile (control), or hydroxyurea (HU) 2 mM for a period of 24, 48 and 72 h. After treatment, cells were suspended in Annexin-binding buffer and stained with Annexin V-FITC conjugate and 5 nM SYTOX Red dead cell stain followed by dual channel flow cytometric analysis. Four sub-populations are identified: Q4: viable ($Annexin\ V^-$ / $Sytox\ Red^-$), Q3: early apoptotic ($Annexin\ V^+$ / $Sytox\ Red^-$), Q2: late apoptotic ($Annexin\ V^+$ / $Sytox\ Red^+$) and Q1: necrotic ($Annexin\ V^-$ / $Sytox\ Red^+$). Quantification of the percentage of cells in each quadrant is shown. A representative plot of three independent experiments is shown.

Fig. 6. Treatment with **1** decreased the clonogenic potential. A) HCT116 cells were plated in 96-well plates and 24 h later were treated with **1** at different doses. After 72 h,

cells were plated in 6-well plates containing drug-free media at different densities ranging from 80-2560 cells per well. After 10 days incubation, colonies were washed with PBS, fixed and stained with crystal violet. Colonies were counted and percentage the surviving fraction was plotted. (B) An image of one representative experiment is shown. The number of cells in each well is indicated.

Fig. 7. P53 tumor suppressor was required for the cytotoxic effect induced by **1**. A) HCT116 cells were treated with **1** at 0.2, 0.4 and 0.8 µM, 1% acetonitrile (control); doxorubicin (DOX) 0.6 µM or hydroxyurea (HU) 2 mM. At 24 and 48 h, samples were collected and processed by Western Blot using specific p53 and p21 antibodies. Actin was used as a loading control. Results are from a single experiment, representative of three independent experiments. B) A co-culture of isogenic HCT116 cells (wild-type, $p53^{-/-}$ and $p21^{-/-}$) tagged with different fluorescent proteins was treated with different doses of **1**. At 6 days, samples were collected and the proportion of each cell population was determined by dual channel flow cytometry. P53 wt ($Mcherry^{+}$ / $iRFP^{-}$); $p21^{-/-}$ ($Mcherry^{-}$ / $iRFP^{+}$) and $p53^{-/-}$ ($Mcherry^{-}$ / $iRFP^{-}$). Data analysis and quantifications for each protein, correcting for loading, was performed using Image Studio software. Quantification of the percentage of cells of each population is shown. For interpretation of the references to color in this figure legend, the reader is referred to the web version of this article.

Table 1
Anti-proliferative effect of **1** on a panel of tumor-derived cells (μM)

Compounds	IC_{50} (μM) values and 95% confidence limits (lower, upper)			
	CCRF-CEM	K562	A549	HCT116
1	1.43 (0.66-3.08)	4.64 (1.63-13.23)	4.27 (0.39-46.64)	0.20 (0.09-0.49)
DOX	0.13 (0.06-0.30)	1.15 (0.52-2.59)	5.12 (1.02-25.7)	0.60 (0.26-1.41)

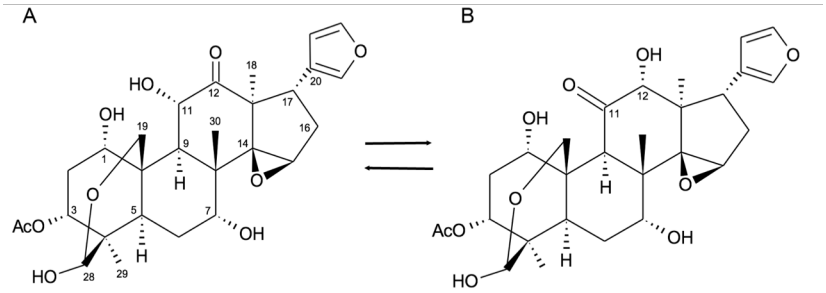

Figure 1

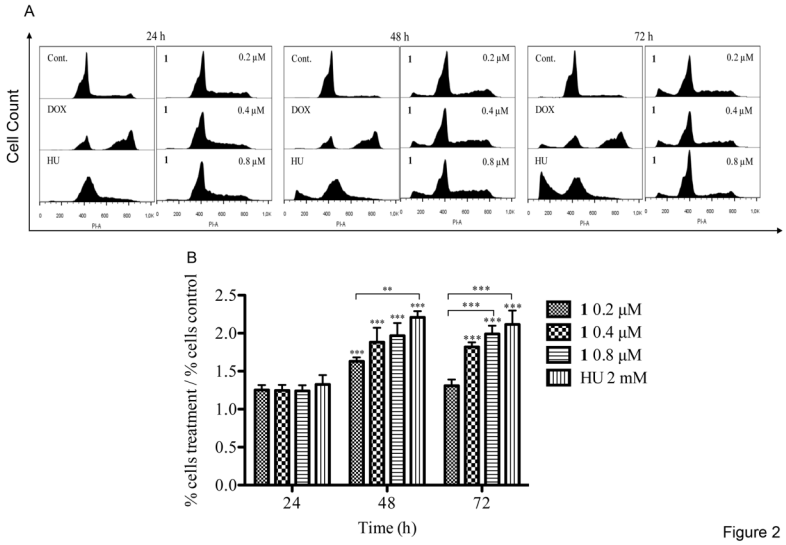

Figure 2

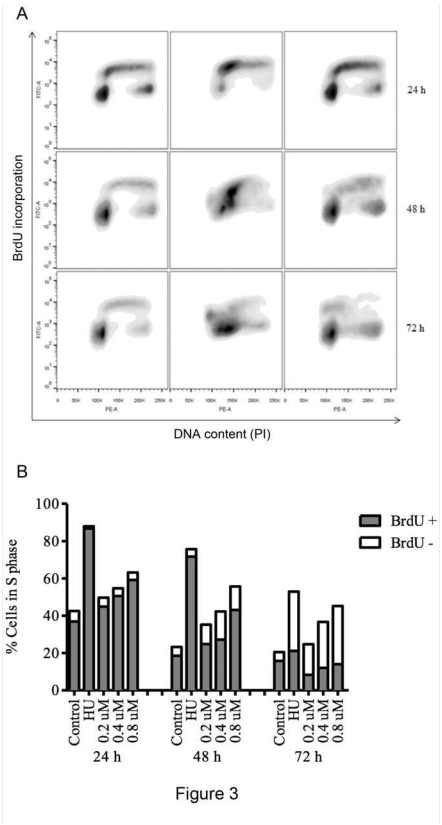

Figure 3

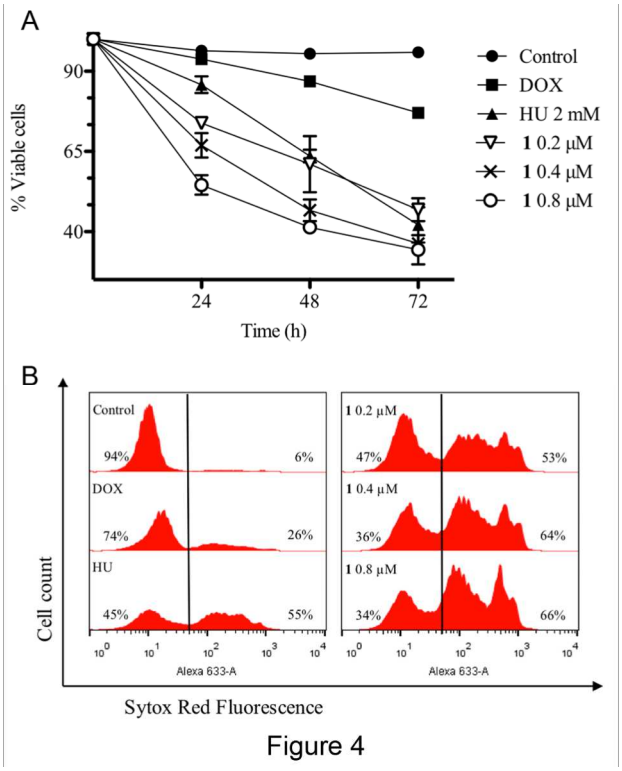

Figure 4

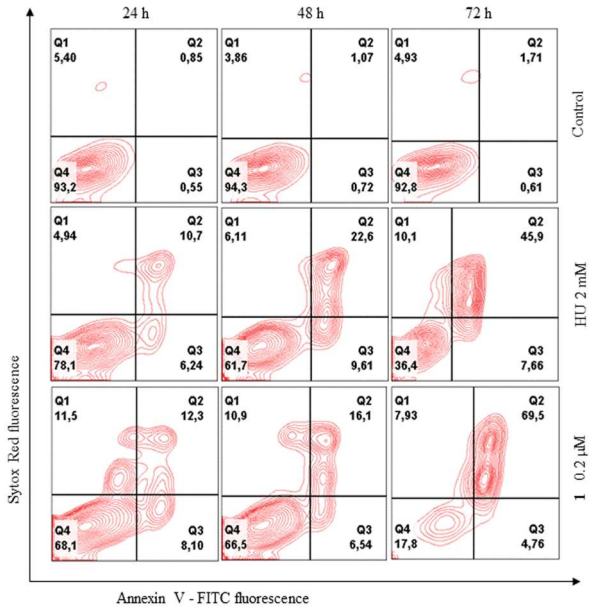

Figure 5

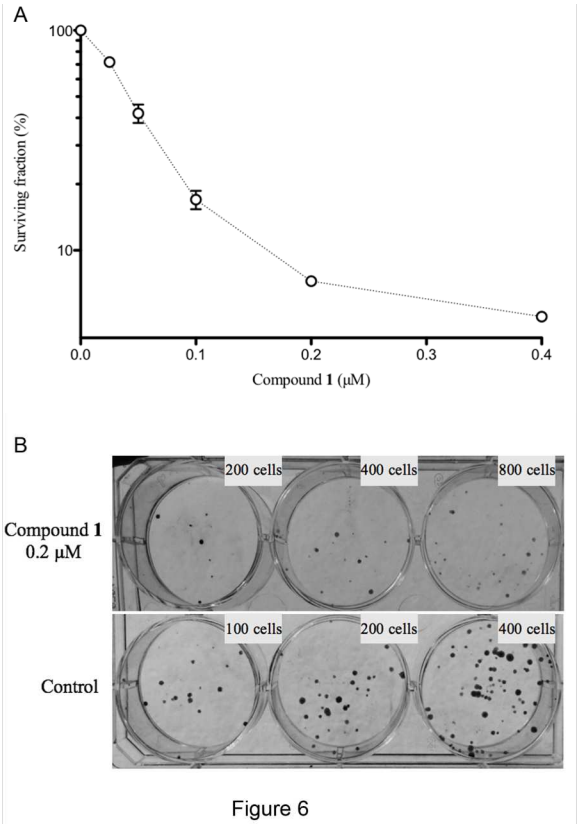

Figure 6

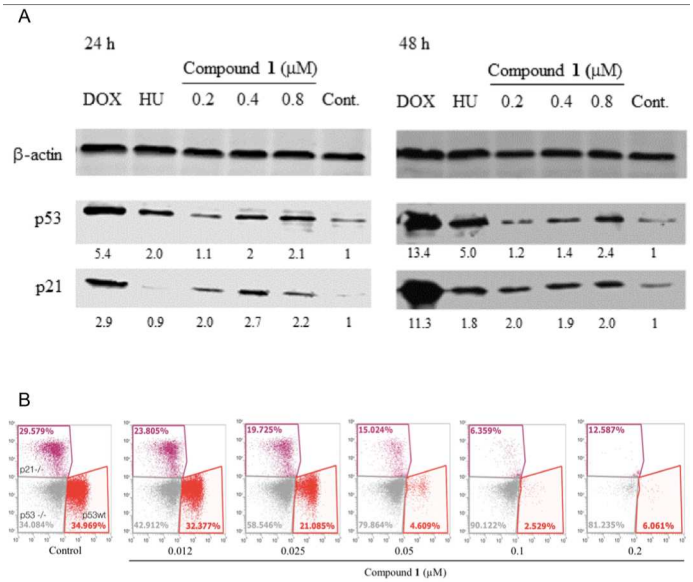

Figure 7